

## Electronic Supplementary Information (ESI)

### Highly Efficient Collection of Underwater Oil Droplet on the Anisotropic Porous Cone Surface via Electric Field

Yufeng Yan,<sup>a</sup> Qiuya Zhang,<sup>a</sup> Yan Li,<sup>a</sup> Zhenyan Guo,<sup>a</sup> Dongliang Tian,<sup>\*a,b</sup> Xiaofang Zhang,<sup>\*c</sup> and Lei Jiang<sup>a,b,d</sup>

<sup>a</sup>Key Laboratory of Bio-Inspired Smart Interfacial Science and Technology of Ministry of Education, School of Chemistry, Beihang University, Beijing 100191, P. R. China. E-mail: tiandl@buaa.edu.cn

<sup>b</sup>Beijing Advanced Innovation Center for Biomedical Engineering, Beihang University, Beijing, 100191

<sup>c</sup>School of Mathematics and Physics, University of Science & Technology Beijing, Beijing 100083, P. R. China. E-mail: xfzhang926@ustb.edu.cn

<sup>d</sup>Technical Institute of Physics and Chemistry, Chinese Academy of Sciences, Beijing 100191, P. R. China

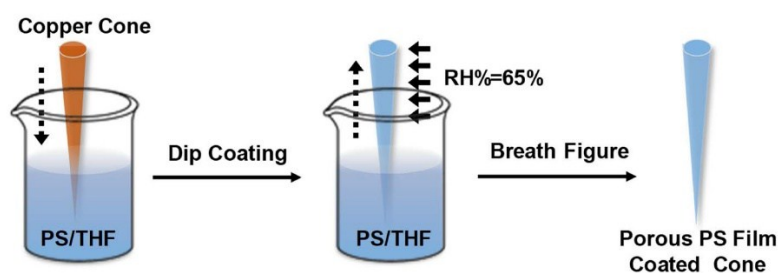


Figure S1. Schematic fabrication process of the porous PS-coated cone via breath figure method. The copper cone is pulled out of 6 wt% PS/THF solution at a certain speed with the humidity of 65%.

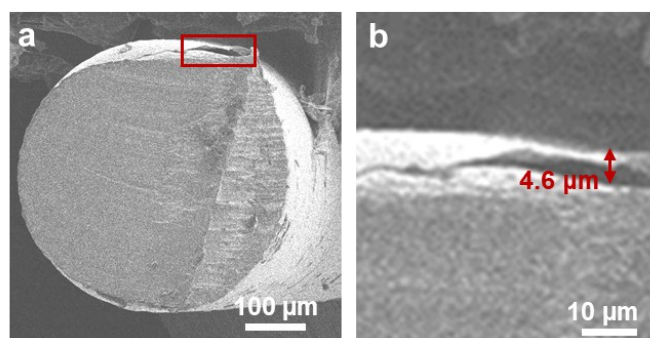


Figure S2. Morphology characterization of porous PS film-coated cone. (a) Scanning electron microscope (SEM) images of cross section of PS film-coated cone. (b) Enlarged view of the region indicated by a red rectangle in part (a). The result show that the cone surface is covered by a PS film with a thickness of  $\sim 4.6 \mu\text{m}$ .

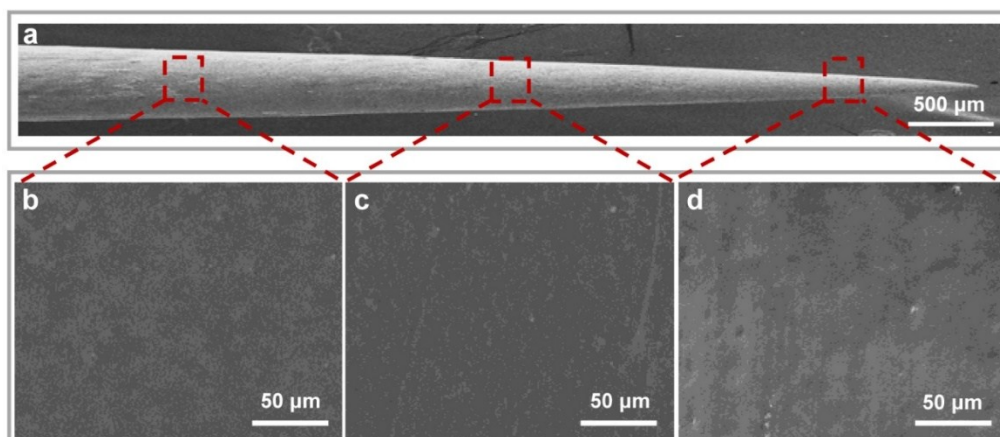


Figure S3. Morphology characterization of the prepared flat PS-coated cone. (a) Scanning electron microscope (SEM) images of flat PS-coated cone ( $2\alpha=4^\circ$ ). (b-d) Magnified SEM images of microscopic morphology on the flat PS-coated cone's bottom, middle, and tip parts. The results indicate that the PS film is relatively smooth.

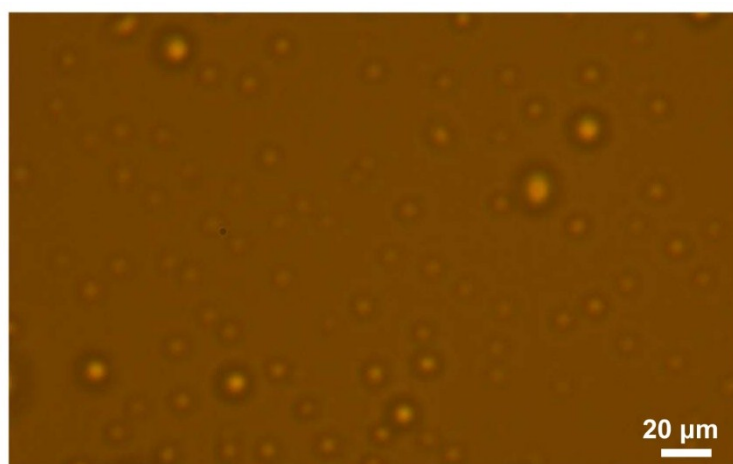


Figure S4. Microscopy image of the micro-sized oil droplets in the oil-water mixture. The largest oil droplet's diameter is smaller than 20 µm.

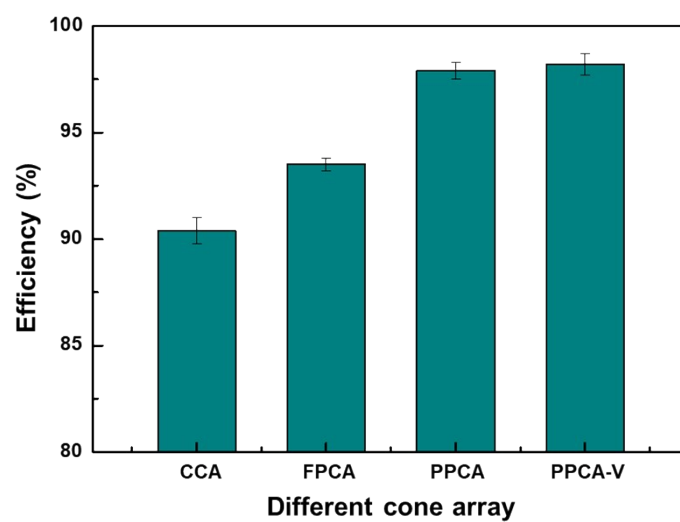


Figure S5 Efficiencies of oil collection on different type cone arrays. The result show that the the porous gradient PS-coated cone array with the applied voltage has a higher oil collection efficiency.

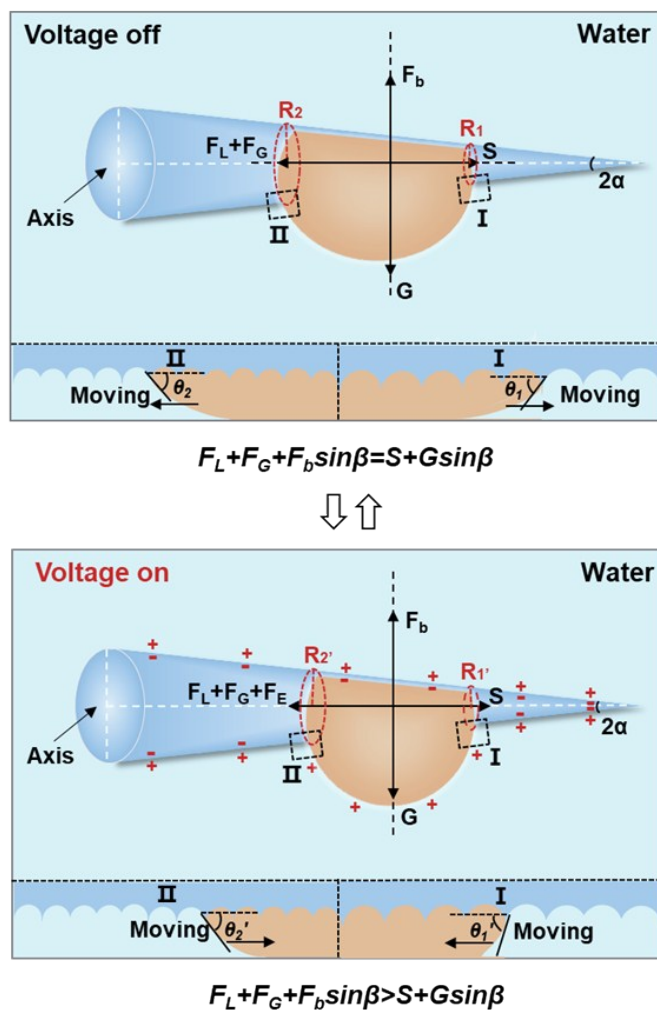


Figure S6. Schematic mechanism of the electric field-assisted oil droplet wetting and dewetting behavior on the underside surface of the cone. For an underwater oil droplet hanging on horizontal cone ( $\theta=0$ ), it can be stably adhered on the porous PS-coated cone in water without an applied electric field owing to the balance force acting on the oil droplet ( $F_L + F_G + F_b \sin \beta = S + G \sin \beta$ ). With applied electric voltage increasing, the electrocapillary pressure induces the oil droplet loses its force balance ( $F_L + F_G + F_b \sin \beta > S + G \sin \beta$ ), the three-phase contact line contracts and oil dewetting process occurs, but the oil does not move on the cone surface. When the voltage is withdrawn, the CAs of oil droplet can be back to the initial state ( $F_L + F_G + F_b \sin \beta = S + G \sin \beta$ ). The results indicate that the oil droplet wetting and dewetting behavior can be reversibly transformed with the varying electric field.